

# Mechanism of Breakdown of Laboratory Gaps

C. F. WAGNER  
FELLOW AIEE

A. R. HILEMAN  
MEMBER AIEE

THE AUTHORS' primary interest in the mechanism of gap breakdown is in its relation to lightning stroke phenomena. In considering the effect of the lightning stroke upon transmission lines, the problem has been resolved into two parts. The first of these is the electrical response of the line to specific assumed stroke characteristics. A method<sup>1-3</sup> to determine this response was recently presented before the AIEE in which it was shown that the time change in the charge in the stroke above the tower may be as important as the current fed into the transmission line. The second part of the problem is the determination of those stroke characteristics that are required to implement this approach. An initial effort<sup>4</sup> along this line was previously presented in which an attempt was made to synthesize the stroke characteristics by correlating the known stroke characteristics with laboratory determined characteristics of long sparks. A further effort<sup>5</sup> was made to utilize the available information concerning the electric field produced at remote points to determine the wavefront of the stroke current. The purpose of this paper is to present a review of available information on laboratory-produced sparks, to present new data on this subject, and to co-ordinate the external manifestations of gap breakdown from an engineering point of view. These results have been co-ordinated in a companion paper,<sup>6</sup> in this issue, with similar data from natural lightning.

## General Phenomenon

In order to establish the general nature of the phenomenon the experiments of Park and Cones<sup>7</sup> will be described first.

sulated plate was mounted to which voltage was applied. Some of their data were obtained with a  $0.07 \times 100\text{-}\mu\text{sec}$  (micro-second) wave which may for all practical purposes, be regarded as a rectangular wave. The crest of this applied wave was held constant at 145 kv, and conditions in the gap were varied by changing the gap length by raising or lowering the sphere. The current flowing from the sphere was measured by means of a cathode-ray oscilloscope and the setup was housed in a black box to expedite photographing the discharge.

Fig. 1 shows a replot of the current from the sphere as this substantially rectangular wave was applied to gaps of various lengths. Some liberty was taken by the authors to line up the large current pips as this illustrates the phenomenon more clearly. Small distortions of time scales result from this procedure. The time of application of voltage is indicated by the small current ripple just

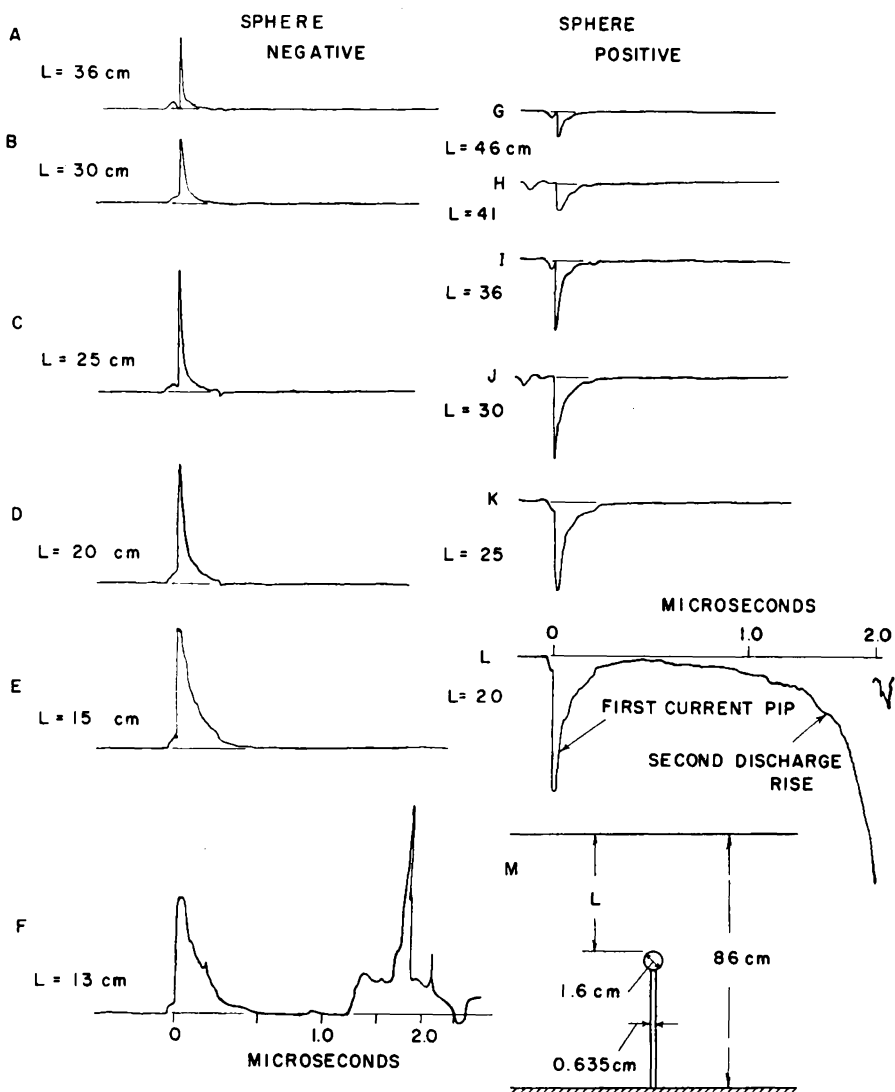


Fig. 1. Currents<sup>7</sup> resulting when an  $0.07 \times 100\text{-}\mu\text{sec}$  145-kv impulse is applied to the gap setup as shown in M

Paper 61-489, recommended by the AIEE Transmission and Distribution Committee and approved by the AIEE Technical Operations Department for presentation at the AIEE South East-South Central District Meeting, New Orleans, La., April 5-7, 1961. Manuscript submitted January 9, 1961; made available for printing March 3, 1961.

C. F. WAGNER and A. R. HILEMAN are both with the Westinghouse Electric Corporation, East Pittsburgh, Pa.

The authors wish to acknowledge the valuable assistance of P. H. Long, J. Brado, and L. Kalining for performing the gap breakdown tests and of H. L. Smith for the computer coding of the channel velocity equations for rapid and accurate determination of the gap time-lag curves.

preceding the almost vertical current change which represents the charging current to supply the electrostatic field before the gaseous discharge phenomenon occurs. The large abrupt change is termed the "first current pip" by Park and Cones. Generally the current pip does not coincide with the instant of application of voltage but is somewhat delayed. The delay is occasioned by the chance occurrence of a free electron coming within the overstressed region in the vicinity of the sphere and triggering the discharge. This is usually called the "statistical time delay" as it depends upon a chance occurrence. The crest of the first current pip for the sphere positive decreases from 18 amperes for  $L=22$  cm as the gap is increased and for the sphere negative from 20 amperes for  $L=10$  cm. The magnitudes vary over wide limits. The current rises to crest in about 0.01  $\mu$ sec and then drops somewhat exponentially to zero in about 0.3  $\mu$ sec for the sphere either positive or negative.

The current ceases after the disappearance of the first current pip at larger gap settings but with the smaller gaps, such as  $L=20$  cm, for the application of the positive potential Fig. 1(L) shows that after the current almost decreases to zero it slowly rises again becoming more rapid and is finally limited by the constants of the circuit. The oscillogram does not

record the final current as a protective gap short-circuited the oscillograph element. This rise in current has been termed by Park and Cones the "second discharge rise."

The first current pip is approximately the same for the application of a negative impulse wave, except as to magnitude, as that obtained for an applied positive impulse, but the second discharge rise is not as gradual in its change and has steeper rates of rise. In each case after the second discharge rise has begun, complete breakdown follows unless the voltage wave is chopped.

#### POSITIVE DISCHARGES

The photographs exhibit different characteristics for positive and negative discharges. Since the discharge is the simpler with the sphere positive it will be described first. For the longer gaps the photographic evidence indicates that streamers that produce light radiate from the sphere but do not complete the passage of the gap. As the gap is reduced to 25 cm some of the streamers do complete passage but the current still drops to zero and breakdown does not occur. For  $L=20$  cm complete breakdown occurs. Photographs taken when the waves were chopped by means of a parallel gap show that the appearance of the discharge begins to change after the second discharge

rise starts. This change consists of one or more bright discharge channels that start at or near the sphere. These discharges have been termed "channels" by Park and Cones to distinguish them from the first kind of discharge which they termed "streamers." These channels move in zigzag fashion across the gap. The length of the channel as a function of time was measured from the progress of the photographed tip and is shown in Fig. 2.

To form a working thesis on which to base discussion the following explanation similar to Park and Cones' is offered to describe the phenomenon. There is no space charge in the interelectrode space prior to initiation of the discharge. The charge on the sphere is determined by the electrostatic solution for the particular configuration. The field is strong near the sphere and decreases as the plane is approached. If the gap spacing is sufficiently small, a zone in the vicinity of the sphere is stressed beyond the critical value of about 30,000 volts per cm. As a free electron appears in this overstressed zone, streamers form which radiate from the sphere. The streamers are not uniform in length and with a sufficiently large gap none reaches the plate. The net effect of the streamers is to produce a space charge that develops its own field and potential drop. Since the applied voltage across the gap is constant, as the space charge develops, less potential is available to produce the charge on the sphere. Consequently the electric field adjacent to the sphere decreases until it reaches 30,000 volts per cm at which point further supply of current is inhibited. The net result is that when the gap is long, a ball of space charge forms around the sphere. A state of equilibrium is attained for which the formation of the space charge is arrested and ionization processes cease. If the gap is decreased and an impulse is reapplied a new state of equilibrium is attained for which the ball of space charge is larger. Finally, as the gap is further decreased, the space charge expands to occupy the entire interelectrode space and, with additional reduction, conditions become conducive to the development of a channel from the sphere. The discharge is converted from a glow discharge to an arc plasma that begins to grow from the sphere toward the plane at a rate indicated by Fig. 2. The criterion for the critical condition, next to the sphere, appears to be such that a charge distribution will produce an average gradient across the entire gap of about 6,000 volts per cm. Conditions governing the transition from corona to an arc

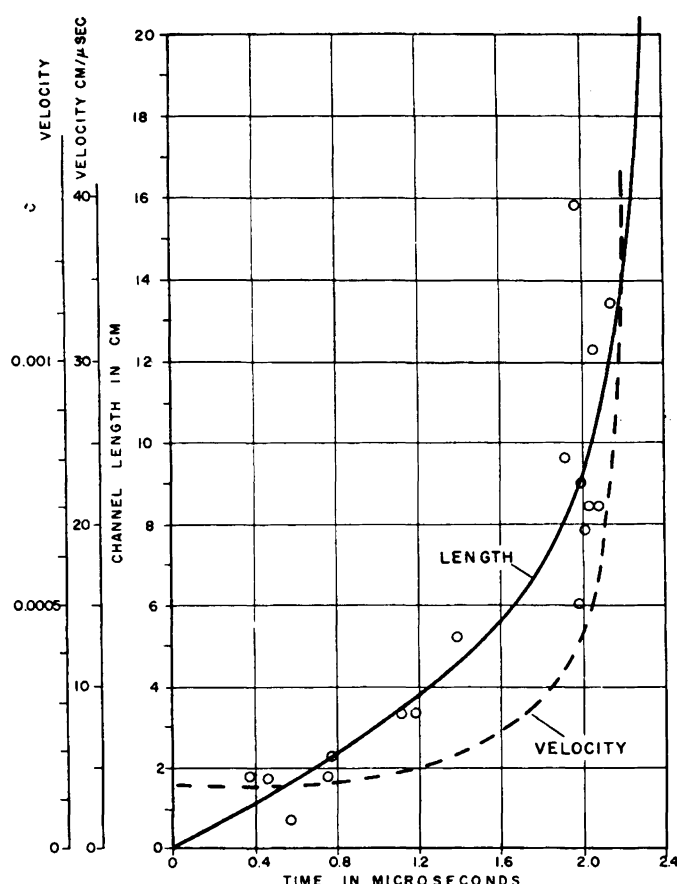


Fig. 2. Progress of channel tip across a 20-cm gap<sup>7</sup> for the conditions of Fig. 1 for the sphere positive. The dotted line is the slope of the distance-time (solid line) curve

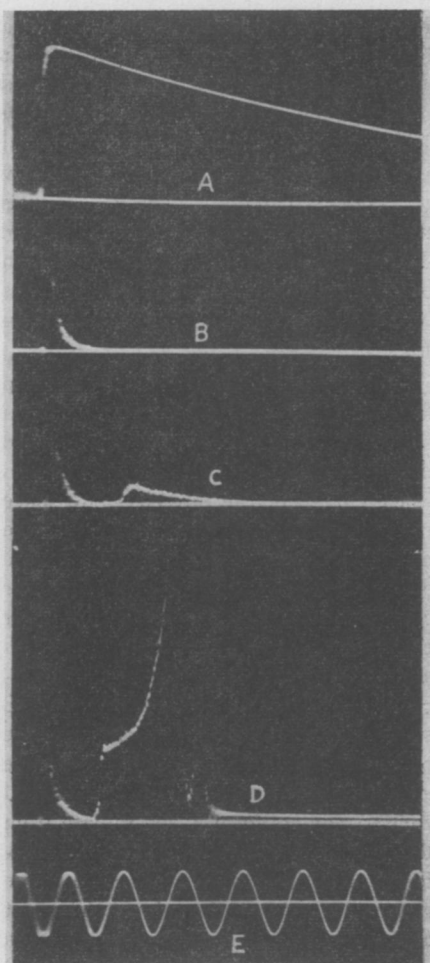


Fig. 3. Current response<sup>13</sup> of a 200-inch rod-rod gap when a  $3 \times 50\text{-}\mu\text{sec}$  3,000,000-volt surge is applied

A—Voltage wave  
B, C, and D—Current waves  
E—Timing wave of 100,000 cycles per second

are not well understood. It is necessary to wait for further developments by the physicist before a more definite explanation can be given. The drop along the plasma channel is very low and thus when it is initiated the effect is progressive as the channel merely constitutes in effect an elongation of the positive electrode. The continually decreasing gap length encourages all the factors originally responsible for the development of the discharge. When the head finally reaches the plate, the channel constitutes a virtual short circuit of the surge generator and the subsequent current is dependent upon the constants of the generator circuit and the characteristics of the arc. This effect is illustrated by the current oscillogram for the 20-cm gap of Fig. 1.

#### NEGATIVE DISCHARGES

With the sphere negative, the charge develops within the interelectrode space in a similar manner, although the actual

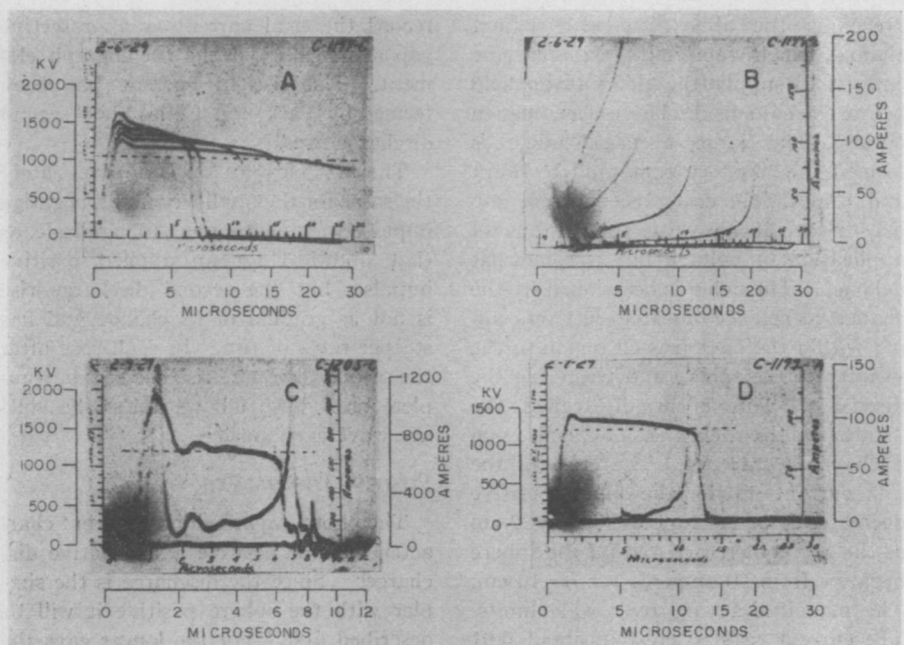


Fig. 4. Sparkover of a 16-unit insulator string equipped with arcing rings of 4-inch-diameter pipe<sup>14</sup>

- A—Five successive applications at increasing voltage
- B—Currents resulting from A
- C—Still higher voltage with corresponding current
- D—Application of voltage and resulting current with the insulators only
- Note the sudden rise of the current prior to the later increase

mechanism of production may be quite different. The negative discharge is more diffuse than the positive both visually and photographically. It consists of numerous streamers of fine texture while the positive discharge consists of fewer but stronger and more crooked streamers.

In the authors' interpretation of the phenomenon just before sparkover it is assumed that the electric gradient, because of the space charge, is approximately constant across the gap although this assumption is not essential to a general understanding of the phenomenon. For the authors' purposes it is convenient to think in terms of an average gradient across the gap. Returning to the Park and Cones experiments, as the gap is decreased and is sufficiently small, the gradient in the interelectrode space due to the space charge increases and the charge density next to the sphere is higher than at the plane. But the conditions necessary to initiate a channel from the positive plane are reached prior to the conditions necessary to initiate a channel from the negative sphere. So the channel starts from the plane before one starts from the sphere. But as the positive channel progresses from the plane, conditions become more critical at the sphere and a channel is finally initiated from there also. The two channels meet

in mid-gap. From this point the current is again determined by the constants of the surge generator and the characteristics of the arc.

#### DISCUSSION

The general nature of the breakdown of nonhomogeneous gaps, consisting of a corona discharge followed by the development of a conducting channel, has been known from the earliest days of impulse testing. For example, Slepian and Torok<sup>8</sup> in 1929 by chopping impulse waves showed by means of photographs the stages of progress of the discharge and also some indication of the maximum currents. Utilizing a rotating camera Allibone,<sup>9</sup> in 1938, presented an extensive study of discharges in long gaps and established the chronological sequence of the leader followed by a return stroke in the laboratory. He commented upon the absence of a discharge from the plane when the rod of a rod-plane gap is positive. This distinction between the corona starting voltage and the breakdown was recognized as early as 1931 by Goodlet, Edwards, and Perry.<sup>10</sup>

Komelkov<sup>11</sup> in 1947 working with gaps between 10 and 100 cm concluded that the drop in the channels was very low, about 55 volts per cm, and that the gradient in the corona streamers was in the range of 6,000 to 10,000 volts per cm. Saxe and

Meek<sup>12</sup> also concluded that the drop along the channels is small.

Hagenguth, Rohlfs, and Degnan<sup>13</sup> furnished limited evidence on a vaster geometric scale which might be viewed as supporting the general nature of the discharge discussed here. They measured the current flowing in the ground electrode of a 200-inch rod-rod gap when a 3,000,000-volt negative  $3 \times 50\text{-}\mu\text{sec}$  impulse was applied to the free electrode. Fig. 3 is a reproduction of Fig. 12 of their paper. Curve A shows the applied voltage which for this gap was just below critical. With 20 applications of this voltage, nine cases developed a glow that bridged only a portion of the gap and the current in the grounded electrode was as shown by trace B; in nine cases the glow bridged the entire gap and the current was as shown by trace C; and in two cases complete sparkover occurred and the current was as shown by trace D. The magnitudes of the three current pips were remarkably consistent and averaged 7.9 amperes. The duration of the pips was 9  $\mu\text{sec}$ .

As early as 1929 Torok and Fielder<sup>14</sup> measured the predischARGE currents of suspension insulators. Fig. 4 is a reproduction of some of their oscillograms. In all of these records the negative pole was grounded. Fig. 4(D) shows the voltage and the current for flashover of a string of 16 insulators. The delay in current occasioned by the necessity of the correct positioning of a free electron is evident and the resultant current is typical of others that have been presented. Figs. 4(A) and 4(B) are mates; the former shows the applied voltages and the latter depicts the resulting currents as a 16-unit insulator string with an arcing ring of 4-inch pipe was flashed over. Fig. 4(C) shows the same test piece with the application of a still higher voltage. The short-circuit current of the surge generator was most likely about 2,000 amperes. It is not known whether the current trace recorded the true maximum as it may have been limited by the operation of a protective gap placed across the shunt.

Thus with this general background of the phenomenon and limited historical review, a discussion of the component parts of the discharge will be undertaken.

### Corona Streamers and Envelope

It is clear from the foregoing that for impulse voltages in excess of the corona threshold voltage but less than the critical breakdown value, a self-limiting space charge is distributed throughout the inter-electrode space. This charge must in

some manner produce an electric field that inhibits further growth of the discharge.

### AVERAGE ELECTRIC GRADIENT AT SPARKOVER

#### For Positive Discharges

As has been mentioned, Allibone commented on the absence of an upward channel from the plane of a rod-plane gap when the rod is positive. Park and Cones also observed that for the sphere positive the channel proceeded from the sphere completely across the gap. Probably the absence of a channel arising from the plate was most dramatically confirmed by Norinder and Salka<sup>15</sup> in their elaborate photographic investigation of spark discharges. The absence of a complication caused by the formation of a channel from the plate insures a somewhat simpler analysis for this type of discharge and for this reason the rod-plane discharge with the rod or small sphere as positive electrode will be considered first.

After a voltage is applied across a gap, the space charge expands and becomes more intense until the gradient next to the electrode drops to 30,000 volts per cm as was mentioned earlier. When the radius of the rod of a rod-plane gap is small, then only a small (in the limit zero, for a pointed electrode) potential is required to produce a charge on the electrode that will result in a gradient at the electrode of 30,000 volts per cm. Then practically all of the applied voltage is

available to produce the space charge. For these cases, when the gap is adjusted so that the corona space charge envelops the entire interelectrode space, the applied voltage divided by the gap length is the average gradient along the axis of the corona envelope.

Once the channel has begun to form the discharge develops to ultimate sparkover almost invariably. For the critical sparkover voltage, half of the applications of voltage produce sparkover. Consequently, this voltage constitutes a measure of the average gradient of the space charge to produce sparkover because the cases that do not cause sparkover represent the maximum development of the space charge without the formation of a channel.

In Fig. 5 the average critical sparkover gradients of rod-to-plane and rod-rod gaps from different sources for both polarities are plotted. The positive polarity data are indicated by the full lines. The Bellaschi and Teague<sup>16</sup> data represented the full wave ( $1.5 \times 40\text{-}\mu\text{sec}$ ) critical sparkover values and were made on gaps up to 200 cm. Breakdown occurred at about 8  $\mu\text{sec}$ . The Hagenguth Rohlfs, and Degnan<sup>13</sup> data covered an even greater range up to 640 cm with an impulse wave of  $3 \times 50\text{-}\mu\text{sec}$ . They stated further that their unpublished data, with gap spacings up to 50 feet tended to give average gradients of the same value. The Gorev, Zalesky, and Riabov<sup>17</sup> data,

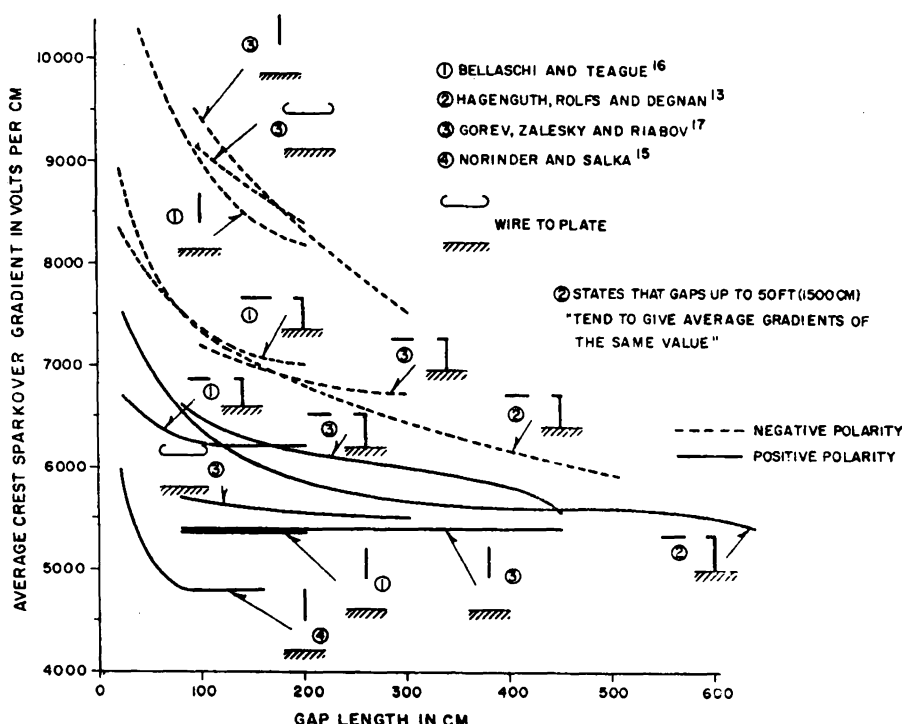


Fig. 5. Average crest impulse sparkover gradient for both positive and negative polarity for gaps of different configuration as a function of gap length

with  $1.5 \times 40\text{-}\mu\text{sec}$  impulse waves, agreed quite closely with the other data. The Norinder and Salka<sup>16</sup> curve for the rod-plane sparkover was only 11% below that of the others. The curves marked by a small horizontal line with curled-up end represent horizontal wire-to-plane data. They agree almost exactly with the rod-plane curves. These curves indicate a practical working average of the average crest sparkover gradient for long gaps of about 5,400 volts per cm for rod-plane gaps and about 6,000 volts per cm for rod-rod gaps which can also be interpreted as the average gradient along the axis of the gap produced by the space charge.

Part of the discrepancy between the laboratory data may be ascribed to differences in waveshape of the applied voltages as well as differences in methods of impulse measurements and to laboratory and observational conditions. Berger's CIGRE report,<sup>18</sup> which discussed comparative tests by 14 different laboratories, indicated that the critical sparkover voltage gradient for a 45-cm rod-rod gap for positive polarity gave a range of from 6,000 to 7,600 volts per cm even after air density corrections had been taken into consideration.

#### For Negative Discharges

In Fig. 1 the waveform of the first discharge pip has approximately the same waveshape for both polarities but the magnitude for positive polarity is somewhat larger than for negative polarity. A corresponding difference in the relative charge for positive and negative applied voltages supplied to the corona envelope of a cylindrical conductor above a plane when impulse has also been noted by Wagner and Lloyd.<sup>19</sup>

As mentioned previously a fundamental difference does exist when a rod-plane gap is impulsed by a negative potential and when impulsed by a positive potential. This difference is the appearance of local discharges at the plate after the negative corona space charge has developed to some extent. One of the plate discharges finally develops into a plasma channel that grows toward the rod before a channel develops from the rod. Because of the presence of the discharges from the plate, the sparkover curves cannot be used directly to determine the average gradient that leads to development of a plasma channel from the rod. One wonders at what value of average gradient would a negative space charge develop into a channel from the cathode if the space charge were permitted to form from the cathode without interference of a corresponding discharge from

the anode. During the initial stages of the channel growth the velocity of the channel is small as compared with the later stages. As the head of the channel progresses, the space charge tends to develop ahead of it. The initial channel development from the anode merely serves to shorten the gap length and increases the gradient adjacent to the cathode to a point where a cathode channel will form. The influence of the anode channel on the cathode channel should be proportionately less for the long gaps than for the small gaps and should be less for a plane anode than for a rod anode. So, in order to estimate the average gradient at which channels are developed, one should refer to the sparkover data for rodplate gaps for long spacings, and make some allowance for the development of the channel from the plate. From Fig. 5 the critical average gradient at which the negative channel develops is estimated to be 8,000 to 9,000 volts/cm.

#### TIME TO ESTABLISH THE CHARGE

Most photographs of the predischarges (used merely to apply to that which occurs before the production of the conducting channels) show very pronounced streamers of high light intensity. The head of some of these streamers travel at very high velocities. For example, Park and Cones stated that the mean streamer velocity was found to be 500 cm per  $\mu\text{sec}$  or 1.7% the velocity of light for the sphere negative and 800 cm per  $\mu\text{sec}$  or 2.3% the velocity of light for the sphere positive. The average deviation was 90 for the sphere negative and 100 for the sphere positive. However, these numbers cannot be viewed as the actual rate at which charge was developed in the inter-electrode space. Some other mechanism must have been present which the physicist may help to explain. As mentioned by Park and Cones, the streamers "should be thought of as a traveling wave of high charge density which is propagated by a process in which new charges are continually produced at the leading surface of the ball by the high gradient there. In the path behind the ball there is left a high concentration of both positive and negative ions, with an excess of positive ions in case the sphere is positive and an excess of negative ions in case the sphere is negative." The shape of the current wave of the first discharge pip is quite repeatable for the sphere positive and somewhat less repeatable for the sphere negative. The average waveshape rises to crest in about 0.008  $\mu\text{sec}$  and decays approximately exponentially to half value in about 0.08  $\mu\text{sec}$ . As Fig.

1 indicates, the time to reach zero is about 0.3  $\mu\text{sec}$ . The waveshape stays essentially constant for both polarities, for all gap spacings, and for fast and slow applied voltage waves.

Remembering that in Park and Cones' experiments the applied voltage was kept constant and the gap conditions were varied by changing the gap length, the fully developed discharge will be taken as that for which a  $0.07 \times 100\text{-}\mu\text{sec}$  positive wave produced 50% sparkovers. From their data this was 24 cm for positive polarity. The effective velocity of charge formation for the positive space charge,  $v_s^+$  will then be defined as the velocity obtained by dividing the half gap length by the time required to produce the fully developed field. Thus

$$v_s^+ = \frac{24}{2 \times 0.3 \times 10^{-6}} = 4.0 \times 10^7 \text{ cm per sec} \\ = 0.0013c \quad (1)$$

For the negative polarity, the effective velocity of charge formation is

$$v_s^- = \frac{11.5}{2 \times 0.3 \times 10^{-6}} = 1.9 \times 10^7 \text{ cm per sec} \\ = 0.0006c \quad (2)$$

The paper by Hagenguth, Rohlfs, and Degnan<sup>18</sup> provided another factor. At the critical sparkover point of a 200-inch rod-gap with a negative impulse applied to the free rod, the time required to develop the space charge was about 9  $\mu\text{sec}$ . This corresponds to a velocity of

$$v_s^- = \frac{200 \times 2.54}{2 \times 9 \times 10^{-6}} = 2.8 \times 10^7 \text{ cm per sec} \\ = 0.0009c \quad (3)$$

Considering the wide range in gaps, from 4.3 to 200 inches, to which these values applied it is remarkable that these numbers are so very nearly equal.

Concerning the actual physical process involved in the establishment of the space charge, it will be observed that the electron drift velocity in a field of 30,000 volts per cm and a pressure of 760 mm (millimeters) is, from Loeb,<sup>20</sup> about  $1.4 \times 10^7$  cm per sec or 0.0005  $c$ . This field is chosen for comparison purposes because it lies midway between the initial and final fields. This value compares favorably with the values given by equations 1, 2, and 3.

#### CHARGE AND ELECTRIC FIELD DISTRIBUTION WITHIN THE GAP

So far consideration has been given to characteristics of the space charge that are subject to actual experimental determination such as the average critical breakdown gradient and the external current feeding it. Because of the difficulties of measure-

ment, little is known of the actual structure of the charge distribution or of the field distribution. Doubtless these distributions are a function of time. Photographic evidence points to the early development of streamers which may be quite independent of and unaffected by each other. They probably are responsible for ionization phenomena that produce charge separations. The speed with which the space charge develops suggests strongly that its development is associated with the movement of electrons rather than ions for both polarities. In time the movements of these charges produce a mass or aggregate effect in which all the streamers play a part.

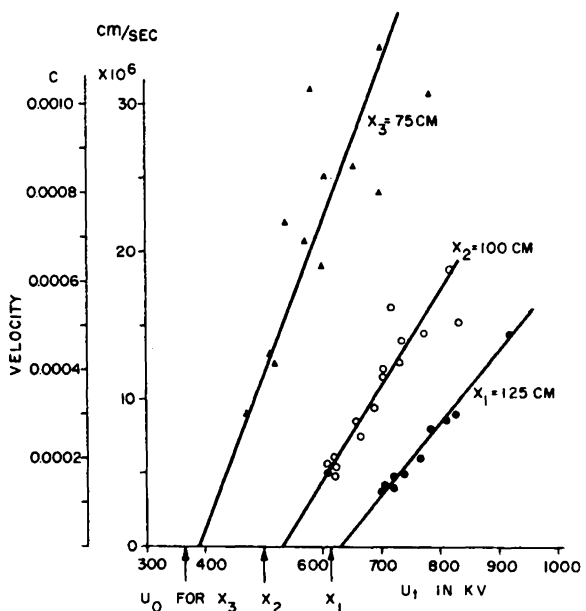
In contemplating the average electric gradient just prior to breakdown, from Fig. 5 for positive polarity, one is immediately struck by the fact that it is constant over a very long range of gap lengths. What sort of charge distribution would give rise to an average gradient that is independent of gap length? Park and Cones suggested a charge concentration that varies inversely as the distance from the spherical electrode in their sphere-plate gap. For either a truly spherical or truly cylindrical charge distribution the resultant electric gradient is a constant. For a rod-plane gap with the rod positive, such distribution can be viewed as being produced by the following mechanism. Suppose that positive ions and electrons are produced uniformly along the numerous very-high-speed streamers that emanate from the positive rod. As the electrons move toward the anode, if the positive ions that are left behind have a uniform radial distribution along each streamer, then the volume distribution would vary inversely with the radius.

The magnitude of the space charge current and the photographs of the discharge both indicate that the mechanism of the negative discharge differs from that of the positive discharge, but the resultant charge distribution may still result in a field that is substantially constant.

#### INTERIM SUMMARY

It appears that if a rectangular voltage is applied across a nonuniform gap whose average gradient is just less than the values given in Fig. 5, a self-limiting space charge develops that inhibits further flow of current. The flow of the charge into the gap is at a rate of about  $0.001 c$  which corresponds approximately to the electron drift. Park and Cones' data show that for 10- to 20-cm gaps this development requires about  $0.3 \mu\text{sec}$  for its completion and in the Hagenguth, Rohlfs, and Degnan data about  $9 \mu\text{sec}$

**Fig. 6. Velocity of the leader development as a function of the terminal voltage,  $u_t$ , for three different constant values of the unbridged gap for a rod-plane gap with the rod positive.<sup>21</sup> Gap spacing is 150 cm and series resistance in the circuit is 2,000 ohms**



with a 200-inch gap. With slower rates of rise and an abundance of electrons to trigger the gap, the current supplying the space charge is reduced in magnitude and spread out over a longer time. A considerable gradient exists within the corona envelope and for the positive discharge, just prior to sparkover, the value is about 5,400 to 6,000 volts per cm and about 8,000 to 9,000 volts per cm for the negative discharge.

#### Channels

It has been observed by a number of investigators that the positive discharge from a rod- or sphere-plane gap is much more stable and consistent than the negative discharge. This applies particularly to the development of the channel. Probably this explains why more data are available concerning the positive channel.

#### POSITIVE CHANNELS

Park and Cones<sup>7</sup> presented the data shown in Fig. 2 concerning the progress of the head of the brightly luminous positive channel as it moved across the gap of the setup mentioned previously. The gap was set for 20 cm and a  $0.07 \times t_c$  wave having a crest magnitude of 145,000 volts was applied which was chopped by a parallel gap. The symbol  $t_c$  indicates the time after the first current pip at which the wave was chopped. Corresponding photographs of the discharge showed the distance that the channel had progressed during the chopping time. The slope of this curve is plotted by the dotted line and indicates that the initial velocity is  $3 \times 10^6$  cm per sec or  $0.0001 c$  which rises slowly at first and

then more rapidly. According to Park and Cones, at midgap (10 cm) the rate of growth is about  $20 \times 10^6$  cm per sec or  $0.0007 c$ .

Akopian, Larionov, and Torosian<sup>21</sup> undertook elaborately combined oscillographic and rotating drum photographic tests on rod-plane and rod-rod gaps of 100–200 cm with positive impulse potentials applied to the gap. Thus, they were able to co-ordinate the travel of the head of the channel with the instantaneous value of the terminal voltage. Komelkov<sup>11</sup> had previously demonstrated that the drop in the channel was about 50 volts per cm. Therefore, assuming the drop to be negligibly small, the voltage across the unbridged portion of the gap is identical with the terminal voltage. They showed as indicated in Fig. 6 (Fig. 8 of Akopian, et al.) that for a rod-plane gap with positive potential applied to the rod, the velocity of the head of the channel for a constant value of the unbridged gap varied linearly with the applied voltage. In this figure  $u_t$  is the applied voltage in kv,  $s$  is the gap length in cm, and  $x$  is the unbridged portion of the gap in cm. Curves are drawn for three constant values of the unbridged gap. The velocity rises from zero at a value of terminal voltage  $u_0$  that would produce discharge when applied for some length of time ("prolonged action" according to the language in reference 21). Beyond this voltage the velocity is proportional to the excess of the terminal voltage above this value. The values of  $u_0$  for the three cases are indicated below the abscissa. They also showed that the positions of the straight lines are related and that for rod-plane gaps the following relation for the velocity holds.

$$v = k \frac{u_i - u_o}{x - 0.23x} \text{ cm per } \mu\text{sec} \quad (4)$$

For a rod-plane gap up to 200 cm,  $k$  is about 9 and for individual discharges the coefficient  $k$  may diverge from its mean value within  $\pm 20\%$ . With  $u_o$  known as a function of  $x$  (very nearly linear), the velocity  $v$  and consequently  $x$  can be solved in terms of the applied voltage  $u_i$ . Akopian, Larionov, and Torosian<sup>21</sup> have tested this procedure with applied voltage waves of widely differing shapes with gratifying results.

#### NEGATIVE CHANNELS

The negative channel is much more erratic than the positive channel but, because the experimental results are usually complicated by the presence of positive channels, it is difficult to discriminate between the effects of the two polarities when both are present and in a developmental state. Examination of the channel currents of Fig. 1 reveals that the currents rise more sharply when the sphere is negative. This may possibly indicate a higher velocity for the channel developing from the sphere. It has also been observed photographically that the positive plate channel progressed a considerable portion of the gap before the negative channel started from the sphere. But in spite of this handicap the two channels met in mid-gap. This was possible only if the negative channel traveled with a higher velocity.

Similar evidence has been provided by the experiments of Hagenguth, Rohlfs, and Degnan<sup>18</sup> which were described previously in connection with Fig. 3. In nine out of 20 shots with the same voltage applied, the glow bridged the entire gap without sparkover. In Fig. 11 of their paper a well-defined streamer can be seen "progressing from the grounded positive rod within the glow emanating from the negative electrode." For the particular photograph shown this streamer has progressed about one-fourth or one-third the distance across the gap. "On complete breakdown of the gap (not shown) at the same voltage there is a well-defined split in the spark near the middle of the gap, indicating where the final streamers [in present terminology, channels] emanating from both electrodes, met." This experiment also strongly indicates higher velocity of the negative channels.

Norinder and Salka<sup>16</sup> related similar experience with rod- and sphere-plate gaps. The plasma channels began at the plate (anode) and proceeded toward the rod or sphere electrode. At a considerably later time similar channels emanated

from the rod or sphere and met approximately in the middle of the gap.

#### ROD-ROD GAPS

For rod-rod gaps, channels form from both electrodes. Akopian, Larionov, and Torosian determined that for an electrode separation of 125 cm the velocity with which the channel tips approach each other can be expressed in the relation

$$v = 11 \frac{u_i - u_o}{x} \text{ cm per } \mu\text{sec} \quad (5)$$

where  $u_i$  is again the actual instantaneous voltage in kv across the electrodes and  $u_o$  is the critical voltage in kv of the unbridged gap,  $x$  in cm. They generalized no further than this single gap but did show that this relation produced good results when the applied voltage was varied over a wide range of waveshapes.

Rusck,<sup>22</sup> on the other hand, stated that this approach was not a complete solution because tests made in his laboratory "show that the formula given in the above mentioned paper cannot be utilized on other gaps." He cleverly obviated the complexity of taking photographs of the discharge by simply accepting two important assumptions that are also inherent in the work of Akopian, Larionov, and Torosian. First, that the drop in the channel is negligibly small and consequently the channels can be viewed as extensions of the electrodes, and second,

that the velocity of approach of the channel tips is a function of the instantaneous electrode voltage and the length of the unbridged gap. As a basis for his work it was necessary to determine experimentally the time to sparkover of gaps to a rectangular applied voltage wave. He found that by applying such a wave to irradiated gaps from 10 to 70 cm the time to sparkover,  $\tau$ , could be expressed by the following formula:

$$\tau = \left( \frac{20+10s}{U} \right)^{\frac{1}{2}} \text{ in } \mu\text{sec} \quad (6)$$

where  $U$  is the magnitude of the applied rectangular wave in kv and  $s$  is the gap length in cm. Rusck also stated that because the critical sparkover voltage,  $U_0$ , is approximately a linear function of the distance  $s$ , the time lag can be expressed by

$$\tau = 4.7 \left( \frac{U_0}{U} \right)^{\frac{1}{2}} \text{ in } \mu\text{sec} \quad (7)$$

His relations were satisfactorily utilized for different types of applied waveforms. He warned that his work should be applied to time lags less than 4 to 5  $\mu\text{sec}$ , as incorrect results would be obtained for longer times.

#### Observations by the Authors

If  $u_o$  in equation 5 is explicitly defined as the critical sparkover voltage of a

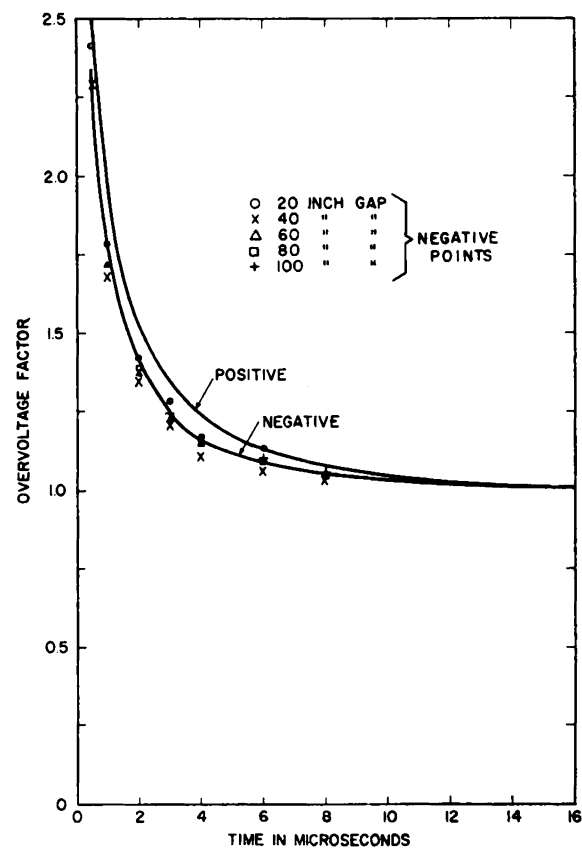


Fig. 7. Time-lag curves for standard rod-rod gaps in response to a  $1.5 \times 40$ - $\mu\text{sec}$  voltage wave for spacings from 20 to 100 inches<sup>23</sup>

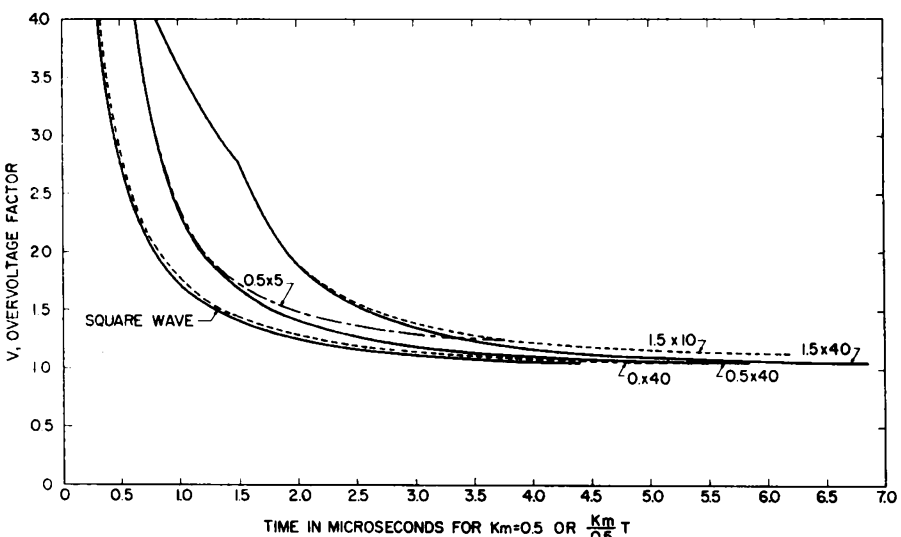


Fig. 8. Calculated time-lag curves for rod-rod gaps for various applied voltage waveshapes

rod-rod gap in response to a rectangular wave and it is assumed that this quantity is proportional to the gap length, then

$$u_0 = mx \text{ in kv} \quad (8)$$

If the difference of the applied waveforms is taken into consideration the factor  $m$  corresponds approximately to the average sparkover value in Fig. 5 in kv per cm. Equation 5 can be rewritten as

$$\frac{dx}{dt} = -k \left( \frac{u_t}{x} - m \right) \quad (9)$$

which merely states that the velocity is proportional to the excess of the average gradient across the unbridged portion of the gap over the critical sparkover gradient. Generally the factor  $k$  will vary with different gap lengths; the negative sign is inserted for analytical purposes so it may be recognized that the unbridged gap decreases when the quantity with the parenthesis is positive. Further transformation of equation 9 is possible to the following:

$$\frac{km}{s} \frac{dx}{dt} = - \frac{\left( \frac{x}{s} \right)}{\frac{1}{m} \left( \frac{u_t}{s} \right) - \left( \frac{x}{s} \right)} d \left( \frac{x}{s} \right) \quad (10)$$

The right-hand side is thus reduced to a per-unit gap length basis.

Rusck's equation 7 which is applicable to rectangular voltage waves applied to 10-70-cm gaps shows that the time lag is independent of the gap length. The work of McAuley<sup>23</sup> with  $1.5 \times 40$  impulse waves on gaps up to 100 inches when replotted in Fig. 7 shows a similar independence of gap length. If, in equation 9,

$$k = Ks \quad (11)$$

then equation 10 is also independent of gap length. This simply means that the

velocities of the channel tips, as will be explained in more detail later, are proportional to the electrode spacings. Some such effect can be expected from the physical considerations involved. Suppose as premised earlier, that in their development the corona streamers deposit a charge density in the interelectrode space, such that at the instant of channel initiation the electric gradient between the electrodes is essentially constant and equal to the value  $m$ . Furthermore, if it is assumed that this space charge is relatively immobile, then as the arc plasma develops within this space,

it forms a good conductor extending as a thin pencil from each electrode. In order to satisfy the condition that the electric gradient along these good conducting pencils is zero, it is necessary that charge be induced along the pencil that will produce an electric field just equal and opposite to that which had existed previously. The induced charge will vary linearly along the pencil and will be proportional to the distance traveled by the tip. The charge density, and consequently the electric field, at the tip will be proportional to the spacing of the electrodes.

Now if a new term,  $V$ , is defined as the overvoltage factor

$$V = \frac{1}{m} \left( \frac{u_t}{s} \right) \quad (12)$$

and equations 11 and 12 are inserted into equation 10, then

$$km dt = - \frac{x/s}{V - x/s} d(x/s) \quad (13)$$

In this same nomenclature, equation 9 expressing the velocity can be changed to the following:

$$\frac{dx}{dt} = -km \left[ \frac{1}{m} \left( \frac{u_t}{s} \right)_x - 1 \right] \\ = -sKm \left( \frac{V}{x/s} - 1 \right) \quad (14)$$

which confirms the previous statement that the velocity is proportional to gap length.

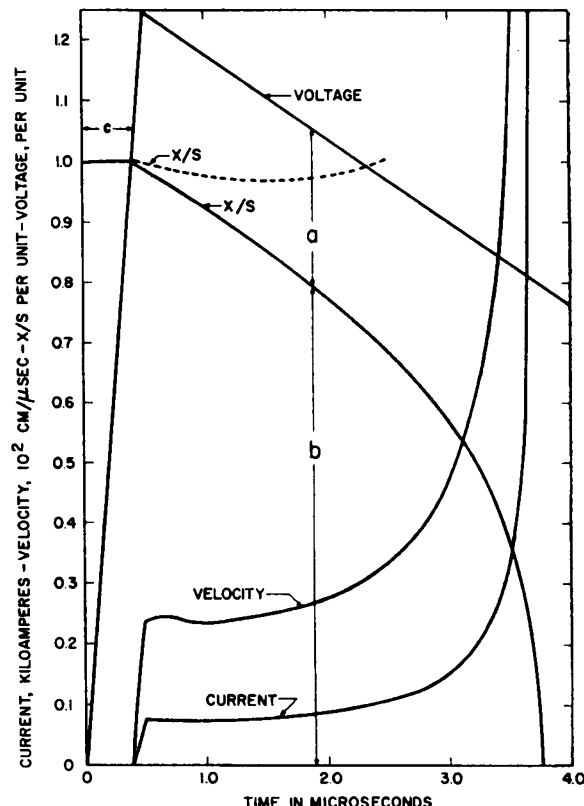


Fig. 9. Determination of the variation of channel velocity, current, and length of unbridged gap with time for an applied  $0.5 \times 5$ -μsec voltage waveshape for a rod-rod gap. Solid line and dotted line  $x/s$  curves for an applied surge with crest overvoltage factors of 1.95 and 1.10, respectively

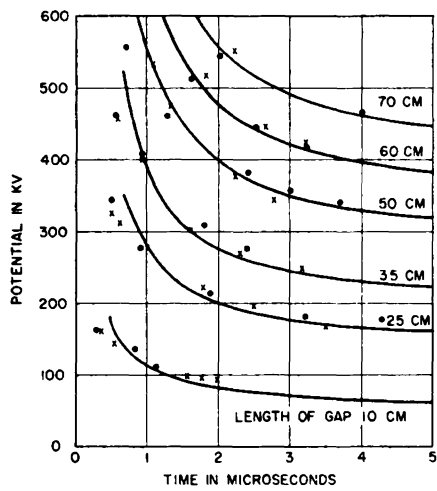


Fig. 10. Calculated time-lag curves for a rod-rod gap with an applied rectangular voltage wave as determined from equation 16 compared with Rusck's<sup>22</sup> test data indicated by the points

X—Positive polarity  
O—Negative polarity

#### APPLICATION TO PARTICULAR WAVESHAPES

With  $V$  known as a function of time, equation 13 permits solution of the determination of the diminution of  $x$  with time. Solutions will be obtained for two waveshapes.

##### Rectangular Wave

With  $V$  constant

$$Km \int_0^t dt = - \int_0^{x/s} \frac{x/s}{V-x/s} d\left(\frac{x}{s}\right)$$

$$Kmt = -(1-x/s) + V \ln \frac{V-x/s}{V-1} \quad (15)$$

and for complete sparkover, the time lag  $T$  is

$$KmT = -1 + V \ln \frac{V}{V-1} \quad (16)$$

The value of  $T$  is plotted in Fig. 8 for  $Km$  equal to 0.5 but the curve is applicable to any value of  $Km$ . This value of  $Km$  was used as it corresponds to a value that, as will be shown shortly, fits the observed test data of Rusck and of Akopian, Larionov, and Torosian.

##### Linearly Rising and Falling Waves

The time lag,  $T$ , for a specific overvoltage factor,  $V$ , for other shapes of the applied voltage is most conveniently determined by using a step-by-step solution of equation 14. One such solution for a  $0.5 \times 5.0$ - $\mu$ sec surge, whose crest overvoltage factor is 1.25, is shown in Fig. 9. The quantity  $x/s$  remains at 1.0 per unit until the applied voltage exceeds an over-

voltage ratio of 1.0 at which time the channel begins its travel across the gap. Therefore, the time denoted by the distance  $c$  is actually a "dead time"; that is, during this time the voltage across the gap is not sufficient to initiate a channel. The total time,  $T$ , for the channel to complete its passage of the gap is 3.8  $\mu$ sec.

Also, the velocity of the channel with respect to time is shown in Fig. 9. The significance of this curve is most easily visualized by rewriting equation 14 as

$$\frac{dx}{dt} = sKm \left( \frac{V-x/s}{x/s} \right) \quad (17)$$

Therefore, from Fig. 9, the velocity for any specific time is the distance  $a$  divided by distance  $b$  multiplied by the constant  $sKm$ . The current curve of Fig. 9 is discussed in a later section.

In Fig. 8 the time lag curves for several waveshapes for  $Km=0.5$  are presented. The overvoltage factor is plotted for other than the rectangular wave as defined by equation 12 except that  $u_i$  is the crest voltage. At sparkover times when  $T$  is less than the front of the wave, the overvoltage factor plotted is the crest voltage actually obtained across the gap. In other words, these curves are constructed and plotted in the same manner as normal time-lag curves. As noted, the time axis can be changed easily for any other value of  $Km$ .

It may be seen in Fig. 8 that the critical voltages vary inversely with the wave tail but are independent of the wave-front. For example, the critical voltage for a  $1.5 \times 40$ - $\mu$ sec wave is about 1.05 and for a  $1.5 \times 10$ - $\mu$ sec wave is about 1.13. However, the critical voltages for a  $1.5 \times 40$ - and a  $0.5 \times 40$ - $\mu$ sec waves are equal. As expected, with small values of time the reverse is true; that is, the front is the

dominant characteristic. Most of the difference in time lags for short times is due to the differences in dead times.

Consider now the critical voltage for a  $0.5 \times 5.0$ - $\mu$ sec wave. According to these calculations and theory, at an overvoltage factor of 1.25,  $T=3.8 \mu$ sec. It was noted in the calculations that for an overvoltage factor of 1.10 the gap did not spark over but channels were initiated. This is illustrated by the dotted curve of Fig. 9 which shows that  $x/s$  starts to decrease when the overvoltage ratio exceeds 1.0. However, because the short wave tail causes a rapid decrease of voltage, the  $x/s$  curve reaches a minimum value, and then rises to its original value of unity.

#### INTERPRETATION OF TEST DATA

Rusck's data are convenient for testing the validity of the relations presented here because he attempted to obtain a rectangular applied voltage wave. It rose to crest in about 0.3  $\mu$ sec and was flat thereafter with the absence of oscillations. Fig. 10 shows his test points for rod-rod gaps of from 10 to 70 cm. There was no appreciable difference between positive and negative polarity. By choosing  $Km=0.46$  and  $m=6.15$  kv per cm, the curves represent the computed results for a rectangular wave. For times longer than 1  $\mu$ sec the agreement is very good, about as good as Rusck obtained with his expression. But below 1  $\mu$ sec Rusck's relation shows a better agreement with tests.

Fig. 11 is a reproduction from the paper by Akopian, Larionov, and Torosian showing the time-lag curves for several different applied voltage waves for a 120-cm rod-rod gap. The relations are the same as used here for which  $k$  or  $Ks$  was

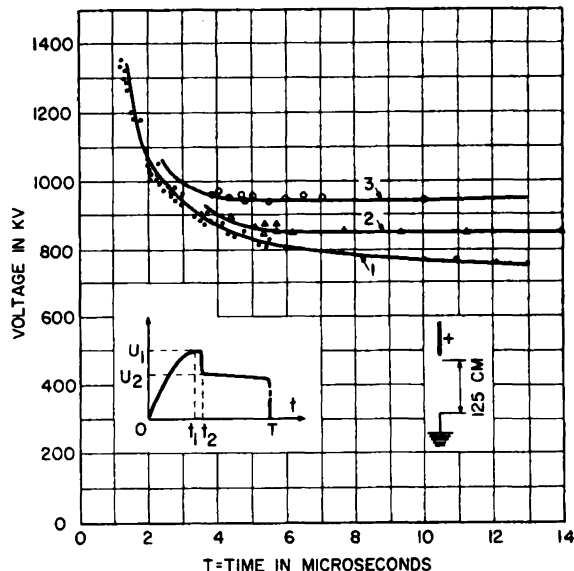
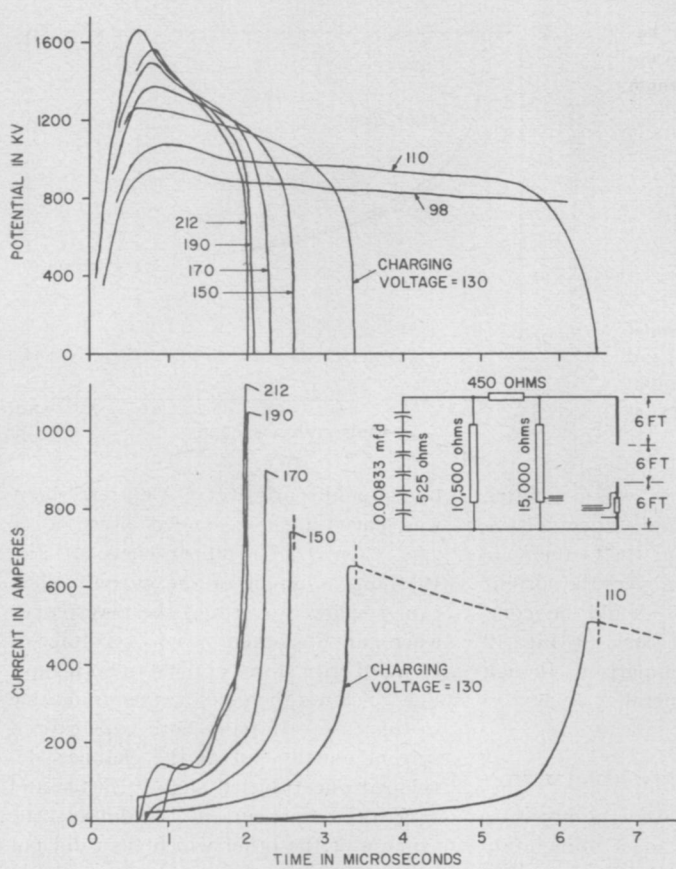
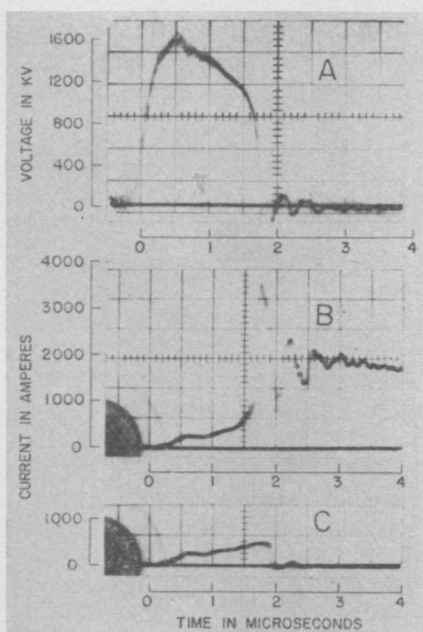


Fig. 11. Time-lag curves for a 125-cm rod-rod gap calculated by equation 5 compared with test data for applied positive polarity voltage waveshapes as illustrated in inset<sup>21</sup>

- 1—Standard  $1.5 \times 40$ - $\mu$ sec wave,  $t_1=2 \mu$ sec
- 2— $t_2=2.9 \mu$ sec; voltage ratio  $u_2/u_1=0.6$
- 3— $t_2=1.8 \mu$ sec;  $u_2/u_1=0.63$



**Fig. 12.** Voltages across and currents through a 6-foot vertical rod-rod gap for positive polarity applied surges. The surge generator charging voltage for critical sparkover is 98 volts



**Fig. 13.** Typical oscillograms of voltages across and currents through two parallel 6-foot rod-rod gaps separated 18 feet. Charging voltage is 200 volts

A—Voltage across gaps  
B—Current through gap which sparked over  
C—Current through gap which did not spark over when other gap sparked over

11. The value of  $K$  is then  $11/125$  or  $0.088$ . From the  $1.5 \times 40\text{-}\mu\text{sec}$  curve the value of  $m$  was estimated as  $720/125$  or  $5.76$  kv per cm. The factor  $Km$  is then  $0.507$  which may be compared with  $0.46$  used in computing the curves in Fig. 13. An average value of  $0.5$  might very well have been used in both Fig. 10 and Fig. 11. The other two curves of Fig. 11 indicated the degree of agreement obtainable with widely different waveshapes. In their computation it is presumed that Akopian, Larionov, and Torosian used the experimentally observed potentials directly across the electrodes and therefore took into account any internal drop that may have existed in the surge generator.

#### Experiments by the Authors

The authors undertook measurement of the current in long gaps under sparkover conditions in order to verify some of the discussed concepts and also to study the factors affecting the current variations, because this is the most important variable to the transmission engineers. A surge generator consisting of  $30 \frac{1}{4}$ -microfarad capacitors was used. Other constants of the circuit are shown in the insert of Fig. 12. In one series of tests a vertical 6-foot  $1\frac{1}{2}$ - by  $1\frac{1}{2}$ -inch rod-rod gap was used. The tip of the lower gap was about 6 feet above the laboratory

floor. The voltage across the gap was measured with a 21,000-ohm compensated voltage divider and the gap current was measured simultaneously by means of a shunt located about midway in the lower rod. Successively higher voltages were applied to the gap by increasing the charging voltage of the generator. The charging voltage is an arbitrary number depending upon the a-c voltage applied to the low-voltage winding of the transformer, which supplies the voltage that is subsequently rectified to charge the capacitors of the generator. However, while arbitrary, it is a quantity proportional to the voltage to which the generator is charged, prior to being discharged into the test circuit. For the critical voltage of the 6-foot gap the charging voltage was 98 volts. The resultant waveshape of the critical voltage is shown in Fig. 12. Increasing the charging voltage resulted in drawing more current from the generator during the discharge process and this current drawn through the resistance of the surge generator resulted in considerable distortion of the voltage across the gap. Figs. 13(A) and (B) are typical oscillograms of the voltage and current. The inductance of the surge generator generally does not play an important role. The oscillation in the current and voltage following completion of the passage of the gap by the arc plasma is caused by the interplay

of the inductance and the capacitance. Its effect has been ignored by estimating the current, when necessary, as the average current during this period.

In Fig. 12 a number of curves of voltage and current for different charging voltages are plotted. Contrary to what might be expected from the theory just presented, current does not begin to flow at just the instant that the critical breakdown voltage is exceeded. The time delay at which current is initiated is longer, the smaller the excess voltage over critical. The delay is made up of two components, first, the period of waiting until a free electron enters the overstressed electrical zones at the two electrodes when the corona streamers that form the space charge are released, and second, the time required for the development of the space charge and conditions propitious for the formation of the channels from the electrodes.

It was impossible in the open conditions of the laboratory to obtain a clean-cut oscillogram of current supplying the space charge just under critical voltage as obtained by Park and Cones<sup>1</sup> and Degnan.<sup>13</sup> Apparently the high free electron concentration caused triggering of the gap on the rising portion of the voltage wave and prevented the sharp rise and exponential decay of the current.

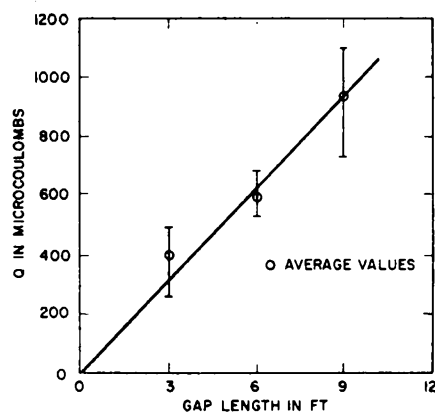


Fig. 14 (left). Relation between the charge fed into the plasma channel and gap length for rod-rod gaps

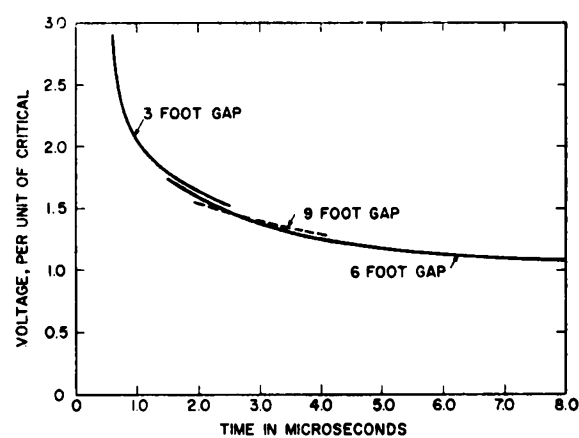


Fig. 15 (right). Experimental time-lag curves for 3-, 6-, and 9-foot rod-rod gaps for applied positive polarity voltages as illustrated

The results obtained did suggest that if the discharge had been delayed a crest of about 25 amperes would have been obtained.

#### CURRENT-TIME RELATION

Saxe and Meek<sup>12</sup> concluded that the current "is proportional to the velocity of the leader stroke." For the present this relation will be accepted and it will be assumed that the instantaneous value of the current,  $i_c$ , is proportional to the instantaneous velocity. Thus,

$$i_c = -K_c \frac{dx}{dt} \quad (18)$$

The negative sign is introduced because as the unbridged gap becomes smaller the sign of  $dx/dt$  must be negative and it is desirable to consider the current as a positive quantity.

If this relation is valid, then upon integrating both sides one arrives at the relation

$$\int_0^T i_c dt = -K_c \int_0^s dx \\ Q = K_c s \quad (19)$$

This states that for any particular value of  $s$ ,  $Q$  should be constant. The area under any one of the curves of current in Fig. 15 to the instant of short circuit is the total charge fed into the channel for a 6-foot rod-rod gap. The range of values thus obtained from Fig. 14 is shown by a bar in Fig. 14. Similar results obtained for a 3-foot and a 9-foot rod-rod gap are also plotted. The slope of this curve gives a value of  $K_c$  equal to 3.2 microcoulombs per cm or amperes per cm per  $\mu$ sec. This linearity serves to confirm the proportionality expressed by equation 18.

Saxe and Meek presented a similar curve obtained with a positive rod-to-plate gap for gap lengths of 8 to 55.4 cm which showed a remarkable linear relation for which the slope was 0.88 microcoulomb per cm. It also bears out the general nature of the phenomenon.

In Fig. 9, the velocity was computed for a  $0.5 \times 5$ - $\mu$ sec wave and an overvoltage factor of 1.25. Applying the factor  $K_c = 3.2$  to this velocity curve gives the current curve indicated. This should be compared with the current curve in Fig. 12 for  $CV = 130$ . The comparison, though not perfect, shows a general agreement in nature.

#### TIME LAG CURVES

With a given surge generator setting having no adjustments made to maintain a particular waveshape, the time lag curves, according to the theory presented here, should be independent of gap length. This happens because as the gap is doubled, then with the same overvoltage factor, the surge generator voltage, the velocity of the channel, and the current and the voltage drop are doubled and the same time lag should result. Therefore, if these relations are correct, the time lag curves plotted against overvoltage factors for 3-, 6-, and 9-foot gaps should form a continuous curve. This is demonstrated to be the case in Fig. 15.

#### PROGRESS OF CHANNELS

Two vertical 6-foot rod-rod gaps were set up 18 feet apart so as not to influence each other electrostatically. When properly adjusted, on application of the surge potential, one, the other, or sometimes

both would spark over. A current shunt was placed in the grounded electrode of gap A only. The upper curve of Fig. 16 shows a replot of the current when gap A sparked over and the lower curve when gap B sparked over as a voltage of 200% of critical was applied to both gaps. Fig. 13 shows the oscillosograms applicable to this case. Initially both gaps carried current equally but as the channels developed one traveled slightly faster and hence drew more current. It did so at the expense of the other which then did not have quite enough current to maintain a corresponding velocity. Furthermore, the first one decreased the unbridged gap and tended to travel even more rapidly than the other. The effect was cumulative and the one to spark over robbed more and more of the current. This effect was pronounced only after the differences in velocities and the lengths of the unbridged gaps became great. While the phenomenon is essentially a resistive one, largely dependent on feeding an appropriate amount of energy into the channel to raise the temperature to those of an arc, undoubtedly charges also rush into the channels as they progress and the fields between the approaching tips increase. But upon contact such charges rush toward each other from the opposing channels through the completed paths. Only an inappreciable amount of this

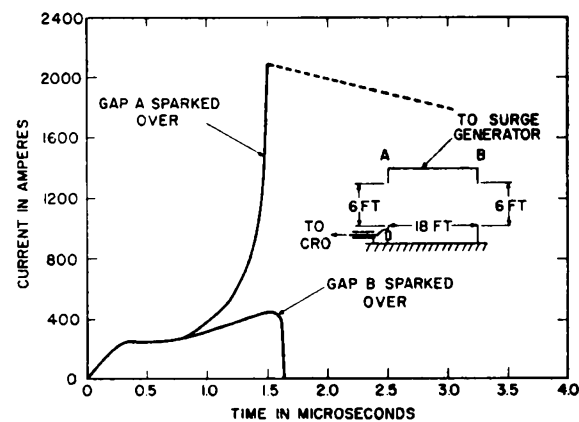
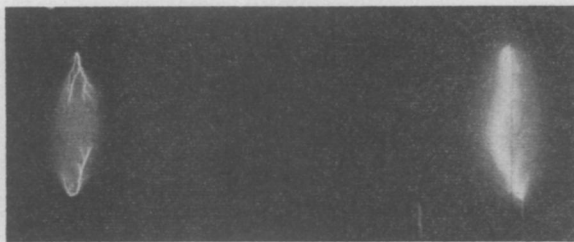


Fig. 16. Current in gap A when gaps A and B are impaled simultaneously. Charging voltage is 200 volts



**Fig. 17.** Channel formation in an unbridged gap when the other gap of two 6-foot paralleled rod-rod gaps sparks over

charge is observed externally as evidenced by the absence of a negative current in the unbridged gap following sparkover of the other gap. Further evidence of this progress of the channels is offered by the still photograph shown in Fig. 17 taken of both gaps simultaneously. Note the extent to which the channels in the gap that did not sparkover have advanced.

#### RING-RING GAPS

A 72-inch-diameter ring made of 2-inch pipe was mounted 94 inches above a 96-inch ring; the latter was located 6 feet above the laboratory floor. Surges of positive polarity were applied with substantially the same surge generator constants as shown in Fig. 12. In Fig. 18 the oscillogram traces of voltages and currents are plotted. The critical sparkover voltage occurred with a charging voltage of 118. The character of the predischarge currents is quite different from and of much greater magnitude than for the 6-foot rod gaps. A very large drop occurs through the resistance of the surge

generator. Neither the  $K$  nor the  $K_c$  constants applicable to rod-rod gaps are applicable to such a gap. The multiplicity of parallel channels apparently affects the fields near the tips of the advancing channels and retards them as compared with the few channels in the simple rod-rod gap. The  $K$  constant was determined only approximately and was found to be about 0.05 to 0.06, which is smaller than that for rod-rod gaps. No further work was done on this gap at this time.

#### PIPE-PIPE GAP

An enlarged form of the ring gap was set up, primarily to simulate a long parallel pipe gap which would have been impossible because of the restricted space of the laboratory. Three 3-inch aluminum pipes each 12 feet long were arranged in triangular configuration about 4 feet from the laboratory floor and a similar set was arranged 6 feet above it. Fig. 19 shows corresponding voltage and current traces. The currents were even larger than for the ring-ring gap. A very pronounced pip occurs at the beginning of the voltage

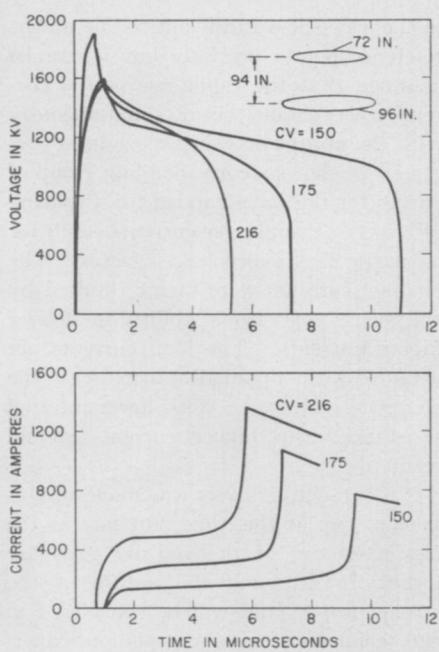


**Fig. 18.** Voltages across and currents through a 94-inch ring-ring gap

traces. These are formed because of the time required for the formation of the space charge. The channel current forms very rapidly and if there were no inductance in the surge generator circuit would increase almost vertically. Simultaneously a corresponding drop in gap voltage occurs. For example, consider the discharge for a charging voltage of 200. The 900-ampere current through the surge generator produces an internal drop of  $900 \times 1,000$  or 900,000 volts. The charge drawn from the surge generator capacitor produces an additional but considerably smaller drop which is directly calculable. Because of the distortions

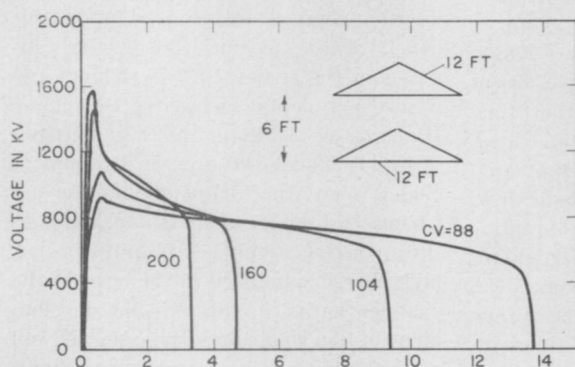


**Fig. 19 (left).** Voltages across and currents through a 6-foot pipe-pipe gap

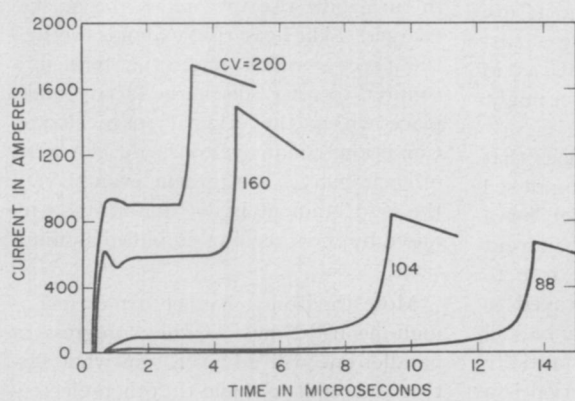


**Fig. 20 (right).** Voltages across and currents through a 3-foot pipe-pipe gap

in the waves it was difficult to line up the reference points precisely but it can be assumed that the rapid rise of the current trace should occur simultaneously with the abrupt drop in gap voltage.

Fig. 20 shows a corresponding group of curves for the same gap set for a spacing of 3 feet. Even larger currents result for a particular overvoltage factor. The channel currents were mainly limited by the surge generator's ability to deliver higher currents. The high currents are attained with only modest increases in the electrode voltages. With lower internal resistance even higher currents should result.

No detailed analysis was made of this type of gap at this time, but just as the characteristics of the rod-rod gaps are useful for studying the nature of the stroke proper, and will be considered in this connection in a companion paper, the characteristics of the large parallel pipe gap will be discussed further in a paper concerning the performance of the transmission line tower. The  $K$  constant was found to be approximately 0.055 to 0.065.

#### ENERGY FED INTO THE DISCHARGE

The instantaneous values of current and voltage from Fig. 12 were multiplied and integrated to give the energy fed into the discharge during the breakdown process. The results of this computation are plotted as circles in Fig. 21 against the short-circuit current,  $I_{sc}$ , of the surge generator. Four additional points obtained 8 months previously, also on a 6-foot rod-rod gap, are plotted by crosses. While more than one channel is involved some portion of the time, the straight line indicates the value of arc energy required to rise the temperature of a pencil of the gaps to arc temperature as  $1.95 \times 10^{-8}$  joules per ampere per cm.

The energy required to develop the arc should be linearly proportional to the short-circuit current and the length of the gap. It is interesting to contemplate whether this is consistent with the relation that the total charge fed into the production of the arc, such as plotted in Fig. 14, is proportional to gap length only. Assuming that a rectangular voltage wave  $V$  is applied to the gap and that  $W$  is the total energy supplied to the gap, then

$$W = VQ \quad (20)$$

If  $R$  is the series resistance, then at short circuit

$$W = RI_{sc}Q \quad (21)$$

and substituting  $Q$  from equation 19

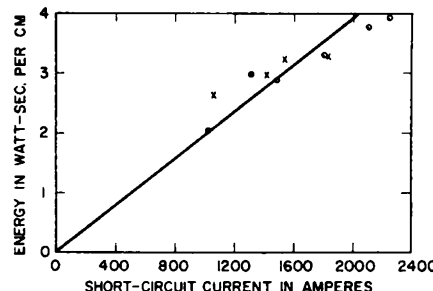


Fig. 21. Energy fed into a 6-foot rod-rod gap

$$W = RK_c I_s s \quad (22)$$

which demonstrates that  $W$  is proportional to  $I_{sc}$  and  $s$ . Since in equation 19 it was assumed that the current is proportional to the velocity, then the linearity of the energy-current relation lends further support to this assumption for rod-rod gaps.

#### General Discussion

The authors have kept their conjectures concerning gaseous electronics to a minimum and have confined themselves largely to the external manifestations of the phenomenon. The physical appearance of the corona discharge alone is ample evidence that the gaseous electronics phenomenon is quite different for positive and negative polarity, but externally they differ only in degree. Nevertheless, the authors wish to comment upon some aspects of the discharge.

It was mentioned in the discussion of the space charge that over a considerable range of gaps a rather definite average electric gradient determines the long-time applied voltage at which sparkover occurs and it further appears that the gradient is constant along the center line of the gap. The work of Akopian, Larionov, and Torosian also indicated this as the channel began to develop when  $u_0$  corresponding to the particular gap was exceeded. By "long time" in this connection they implied a time of the order of 100  $\mu$ sec. With longer times it is quite conceivable that other factors might enter which would alter the nature of the space charge. Thus, for a sustained and continuous potential, as in d-c corona, the charge distribution might be quite different.

It was found by Park and Cones that when a  $0.07 \times 100$ - $\mu$ sec wave was impressed across their sphere-plate gap, set for a length of between 20 and 50 cm, the current that supplied the space charge rose to crest very rapidly and then decayed to half value in 0.08  $\mu$ sec. So it may be said that the space charge is substantially established in 0.1  $\mu$ sec. This period is a

function of the phenomenon occurring within the gap, as the regulation of the circuit is sufficiently stiff that the currents required by the space charge do not produce much drop in the external circuit. While Akopian, Larionov, and Torosian used a somewhat larger external resistance it can be assumed that for the length of gaps and for the rates of rise of voltage they used, there was very little lag between the voltage and the establishment of the space charge. This explains why in their analysis of the time to breakdown the phenomenon could be described in terms of the development of the highly conducting channels alone.

For longer gaps, such as the 200-inch rod-rod of Hagenguth, Rohlfs, and Degnan, the time of space charge formation is significant with respect to the total time to breakdown. It remains to be ascertained whether the time lag curves for different waveshapes for such gaps can be computed in a manner similar to that employed by Akopian, Larionov, and Torosian and amplified in this paper.

The foregoing statements may be not completely valid for conditions near the end of travel of the channel. Here the velocity attains very high values and the space charge may not be able to develop sufficiently to keep pace with the values corresponding to the reduced unbridged gap.

As the good conducting channel advances through the relatively immobile space charge, as has been mentioned previously, charges are induced upon this pencil of arc plasma. From the estimates of the current in the channel and from experiments, such as performed by Higham and Meek<sup>24</sup> on the characteristics of rapidly developed arcs, it can be concluded that the diameter of the arc plasma is approximately 2 mm and that the arc is a relatively good conductor. A high charge is induced in the head of the channel that is conducive to the development of a high gradient laterally as well as ahead of it. This charge and gradient, in turn, give rise to copious corona discharges. The head thus expands through the process which might be termed a counter corona discharge that takes place within the original space charge. Conditions conducive to the development of such charges are present even though the field gradient is not uniform as promised by the foregoing simplified assumptions.

More than one channel can form simultaneously, but as they progress in parallel one will advance somewhat farther and tends to shield the others electro-

statically and thus reduce the field in advance of them. By this process the advance of the others is retarded and this effect becomes progressive. For gap configurations that approach two geometric lines parallel to each other such as formed by two long parallel pipes, this effect should not be as dominant as for a single rod-rod gap. The tests made with two 6-foot rod-rod gaps set 6 feet apart as shown by the insert of Fig. 12, showed that in some cases both gaps sparked over simultaneously which indicates that for separations greater than the gap length the shielding effect is not very great. Tests with smaller separations were not made. Allibone<sup>9</sup> showed that even for two parallel plates two dominant arc paths can form simultaneously.

While more information is available concerning the propagation of channels from the anode than from the cathode, since the process of channel formation is essentially a thermal process, it is expected that the velocity of propagation of the channels from the cathode should be of the same order of magnitude.

## Summary

Upon application of an impulse voltage, of such value as not to cause sparkover, a nonuniform field gap, of the proportions frequently encountered in engineering work, the field at first corresponds to that which would be expected from the conventional electrostatic solution. The fields in the vicinity of the electrodes may exceed the critical field momentarily but when this field is exceeded and a free electron appears in the region of the overstressed field, an electron avalanche is triggered that develops into a space charge. For rod-rod gaps the space charge develops from both electrodes but for rod-plate gaps from the rod only. The flow of the charge into the intervening gap is at a rate of about  $0.001 c$  which corresponds approximately to the electron drift; so that for a 10-cm gap the charge has diffused through the entire gap in about  $0.3 \mu\text{sec}$  and for a 200-inch gap in  $9 \mu\text{sec}$ . The current feeding the space charge rises very rapidly and decreases somewhat along an exponential curve so that a substantial portion of the space charge is established in slightly less time than these values.

A certain critical average gradient exists for gaps which will produce ultimate sparkover of the gap with prolonged application of the voltage. There is some evidence to indicate that when the space charge is fully developed across the

gap the electric gradient in the gap between the electrodes is approximately uniform. The average critical gradients vary between about 5,500 and 10,000 volts per cm depending upon gap configuration and polarity. When the critical average gradient is exceeded a channel is initiated which usually starts from the anode. In the case of a rod-plate gap with the rod positive the channel develops for the entire length of the gap without the development of a plasma channel from the plate. But with the rod negative a plasma channel is first initiated from the plate, and after progressing about half-way across the gap it is met by a more rapidly moving channel, which started at a later time, from the rod. For a rod-rod gap, the plasma channel also starts from the anode and is met in mid-gap by a later initiated channel from the cathode. The drop in the plasma channels is so small that it is considered negligible with respect to the applied voltages concerned in this phenomenon.

For rod-rod gaps, the heads of the two channels approach each other with a velocity that is proportional to the excess of the terminal voltage over the critical sparkover voltage for the instantaneous value of the unbridged gap, and inversely proportional to the length of the unbridged gap. The channels grow with a relatively small initial velocity which is accelerated as the unbridged gap decreases. By using these velocity relations, the time lag of rod-rod gaps can be computed for any applied voltage across the gap. Expressing the applied voltage in terms of the critical sparkover voltage for a rectangular wave, results can be reduced to a per-unit basis that is independent of the length of the gap. These characteristics can be completely described by two parameters.

The channel current is proportional to the velocity of propagation of its head, and therefore can be determined in terms of the instantaneous velocities discussed previously. For small overvoltages, the channel currents are usually concave upward, but for high overvoltages and sufficiently high resistances between the applied voltage and the gap, the current is of a stepped character.

The form of the current wave feeding the initial space charge when a rectangular wave is applied to a gap and the form of the current flowing during the development of the channel is quite opposite; the former decreases somewhat as a negative exponential with time, and the latter increases somewhat as a positive exponential with time. It is shown in the companion paper in this issue that these

contrasting characteristics lead to an explanation of the steps in the lightning stroke.

The fact that the magnitude of the currents feeding the initial space charge are quite small, in comparison with the currents that occur during the plasma channel forming phase and with the short circuit currents permitted by the constants of the surge generators, was appreciated quite early. As shown in the companion paper, the currents occurring during the steps of the lightning stroke are also small in comparison with the currents in the return stroke. The phenomenon appears to be essentially a thermal one; sufficient energy must be injected into the gap in order to raise a thin cylinder of air to arc temperatures.

## References

1. A NEW APPROACH TO THE CALCULATION OF THE LIGHTNING PERFORMANCE OF TRANSMISSION LINES, C. F. Wagner. *AIEE Transactions*, pt. III (*Power Apparatus and Systems*), vol. 75, Dec. 1956, pp. 1233-56.
2. A NEW APPROACH TO THE CALCULATION OF THE LIGHTNING PERFORMANCE OF TRANSMISSION LINES—II, C. F. Wagner, A. R. Hileman. *Ibid.*, vol. 78, Dec. 1959, pp. 996-1021.
3. A NEW APPROACH TO THE CALCULATION OF THE LIGHTNING PERFORMANCE OF TRANSMISSION LINES—III. A SIMPLIFIED METHOD—STROKE TO TOWER, C. F. Wagner, A. R. Hileman. *Ibid.*, vol. 79, Oct. 1960, pp. 589-603.
4. THE LIGHTNING STROKE, C. F. Wagner, A. R. Hileman. *Ibid.*, vol. 77, June 1958, pp. 229-42.
5. DETERMINATION OF WAVE FRONT OF LIGHTNING STROKE CURRENTS FROM FIELD MEASUREMENTS, C. F. Wagner. *Ibid.*, vol. 79, Oct. 1960, pp. 581-89.
6. THE LIGHTNING STROKE—II, C. F. Wagner, A. R. Hileman. *Ibid.* (see pp. 622-42 of this issue).
7. SURGE VOLTAGE BREAKDOWN OF AIR IN A NON-UNION FIELD, J. H. Park, H. N. Cones. *Journal of Research*, Washington, D. C., vol. 56, 1956, pp. 201-224.
8. STREAMER CURRENTS IN HIGH VOLTAGE SPARKOVER, J. Sieplan, J. J. Torok. *Electric Journal*, East Pittsburgh, Pa., vol. 26, 1929, pp. 107-10.
9. THE MECHANISM OF THE LONG SPARK, T. E. Allibone. *Journal, Institution of Electrical Engineers*, London, England, vol. 82, 1938, pp. 513-21.
10. DIELECTRIC PHENOMENA AT HIGH VOLTAGES, B. L. Goodlet, F. S. Edwards, F. R. Perry. *Ibid.*, vol. 69, 1931, pp. 695-727.
11. THE STRUCTURE AND PARAMETERS OF THE LEADER DISCHARGE, V. Komeikov. *Bulletin, Academy of Science, Technical Sciences Section*, No. 8, Moscow, U.S.S.R., 1947, pp. 955-66.
12. THE INITIATION MECHANISM OF LONG SPARKS IN POINT-PLANE GAPS, R. F. Saxe, J. M. Meek. *Journal, Institution of Electrical Engineers*, vol. 102, pt. C, 1955.
13. SIXTY-CYCLE AND IMPULSE SPARKOVER AND LARGE GAP SPACINGS, J. H. Hagenguth, A. F. Robins, W. J. Degnan. *AIEE Transactions*, pt. III (*Power Apparatus and Systems*), vol. 71, 1952, pp. 455-60.
14. IONIZATION CURRENTS AND THE BREAKDOWN OF INSULATION, J. J. Torok, F. D. Fielder. *Ibid.*, vol. 49, Jan. 1930, pp. 352-58.
15. MECHANISM OF LONG-GAP NEGATIVE SPARK DISCHARGES IN AIR AT ATMOSPHERIC PRESSURE, H. Norinder, O. Salma. *Arkiv for Fysik*, Stockholm, Sweden, vol. 5, 1952, pp. 493-529.
16. IMPULSE AND 60 CYCLE STRENGTH OF AIR,

- P. L. Bellaschi, W. L. Teague. *AIEE Transactions*, vol. 53, 1934, pp. 1638-45.
17. IMPULSE CHARACTERISTICS OF LARGE GAPS, A. A. Gorev, A. M. Zalevsky, B. M. Riabov. *Bulletin no. 142*, CIGRE, Paris, France, 1948.
18. REPORT ON THE WORK OF THE STUDY COMMITTEE NO. 8—OVER VOLTAGES AND LIGHTNING, K. Berger. *Bulletin no. 326*, CIGRE, 1956.
19. EFFECTS OF CORONA ON TRAVELING WAVES, C. F. Wagner, B. L. Lloyd. *AIEE Transactions*, pt. III (Power Apparatus and Systems), vol. 74, Oct. 1955, pp. 858-72.
20. BASIC PROCESSES OF GASEOUS ELECTRONICS (book), L. B. Loeb, University of California Press, Berkeley and Los Angeles, Calif., 1955.
21. ON IMPULSE DISCHARGE VOLTAGES ACROSS HIGH-VOLTAGE INSULATION AS RELATED TO THE SHAPE OF THE VOLTAGE WAVE, A. A. Akopian, V. P. Larionov, A. S. Torosian. *Bulletin no. 411*, CIGRE, 1954.
22. EFFECT OF NON-STANDARD SURGE VOLTAGES ON INSULATION, Sune Rusck. *Bulletin no. 408*, CIGRE, 1958.
23. FLASHOVER CHARACTERISTICS OF INSULATION, P. H. McAuley. *Electric Journal*, July 1938, pp. 273-80.
24. VOLTAGE GRADIENTS IN LONG GASEOUS SPARK CHANNELS, J. B. Higham, J. M. Meek. *Proceedings, Physical Society*, London, England, pt. 9, vol. 63, Sept. 1950, pp. 633-648.

## Discussion

H. Baatz and A. Fischer (Studiengesellschaft für Hochspannungsanlagen e.V., Nellingen über Esslingen, Germany): The development of a discharge during the breakdown of rod-rod gaps was investigated. Voltage and current were measured simultaneously by a cathode-ray oscillograph at the high-voltage electrode. The high-voltage electrode was chosen as measuring point so that a single rod, without an opposite electrode, could be investigated. Various forms of rods were used; see Fig. 22. The optical view of the discharge figures were taken, as are Lichtenberg figures, by photographic paper which was held axially between the electrodes.

The vertically arranged rod-rod gap with a distance of 350 mm was investigated mainly. The distance was always the same; the peak value of the impulse voltage was varied. For all oscillograms the impulse voltage of 0.3/40 was used. The 100% breakdown voltages for the distance of 350 mm were approximately +305 kv and -315 kv.

### POSITIVE IMPULSE VOLTAGE

Fig. 23 shows a characteristic oscillogram. At  $t_1$  the first part of the impulse generator fires, and at  $t_2$  the impulse voltage is applied to the gap. During the rise of the

voltage to its peak value,  $U_{max}$ , the capacitive charging current with peak value  $i_{c,max}$  flows. At the moment  $t_{k1}$ , a current impulse which may be called current of impulse corona appears. Its peak value is  $i_{k1}$ . At  $t_{k1}$ , the voltage at the gap is  $U_k$ . This value is the inception voltage of impulse corona. The corona current,  $i_{k1} = i - i_c$ , diminishes as an exponential function. It remains zero for  $U_{max}$  voltages at least 20% below the 100% breakdown voltage  $U_D$  of the gap.

### NEGATIVE IMPULSE VOLTAGE (FIG. 24)

With  $U_{max}$  voltages  $\leq 0.8 U_D$  the oscillograms are nearly the same as Fig. 23 with inception of impulse corona at  $t_{k1}$  and diminishment of the current  $i_{k1} + i_c$  ( $i_c$  capacitive current). Sometimes the current impulse of the impulse corona is totally absent. With voltages  $0.8 U_D < U_{max} < U_D$ , as shown in Fig. 24, a new event which is not seen in the current oscillogram of positive electrodes appears. After the capacitive charging current belonging to the beginning of the impulse voltage has disappeared, sometimes, during the return of the impulse voltage at  $t_{k2}$ , a very steep and high current impulse,  $i_{k2}$ , appears. This occasionally is followed by another, smaller impulse. The impulses disappear as an exponential function. In every case when the discharge develops to breakdown, the current impulse,  $i_{k3}$ , and

sometimes  $i_{k4}$ , may be observed. While they are still present the final rise of current up to the breakdown at  $t_D$ , follows.

The inception voltage  $U_k$  of impulse corona increases slightly with increasing peak value of impulse voltage for all forms of electrodes used. Table I shows the mean values for the different electrodes.

Table I

Electrode	$U_k$ (kv)
1.....	+110..... -85
2.....	+ 96..... -78
3.....	+105..... -95
4.....	+148..... -95

All forms of electrodes used clearly show the growth of  $i_{k1}$  with increasing  $U_{max}$  and therefore with increasing steepness of the impulse voltage. With peak values up to  $U_{max} = 300$  kv,  $i_{k1}$  is directly proportional to  $U_{max}$ ; see Table II.

Table II

Electrode	$i_{k1}/U_{max}$ (Amps/100 Kv)	
	+ Impulse	- Impulse
1.....	2.2.....	1.35
2.....	1.7.....	1.5
3.....	1.75.....	1.25
4.....	3.5.....	2.0

Figs. 25(A) and 25(B) shows oscillograms of voltage and current without breakdown of the gap, and Figs. 26(A) and (B) with breakdown. The total occurrence including breakdown is shown in Figs. 27(A) and 27(B). In Figs. 28 and 29 the corona streamers bridge the whole gap without breakdown. When the breakdown starts the channels begin again at the electrodes. These pictures cannot be reprinted due to blackened photographic paper. In the original photos the formation of the channels is clearly seen.

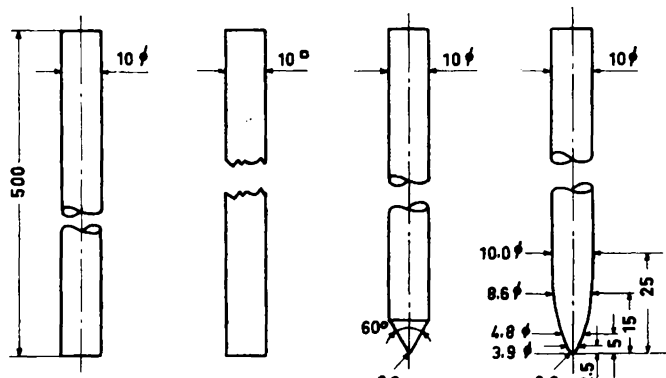


Fig. 22. Various forms of rod electrodes

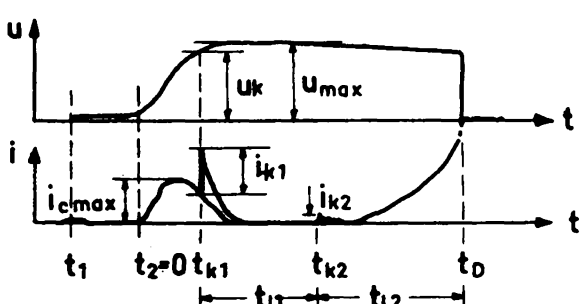


Fig. 23 (left). Characteristic oscillogram with impulse positive

Fig. 24 (right). Characteristic oscillogram with impulse negative

